

# Seismic Site Classification of Recording Stations in Tarai Region of Uttarakhand, from Multiple Approaches

NH Harinarayan · Abhishek Kumar 

Received: 5 June 2017 / Accepted: 28 October 2017 / Published online: 2 November 2017  
© Springer International Publishing AG, part of Springer Nature 2017

**Abstract** Repeated earthquakes (EQs) are clear indication of alarming seismicity which can be witnessed across Indian subcontinent. Increase in population density with inappropriate construction practice repeatedly rise alarm that in comparison to damage scenarios experienced during previous major to great EQs in India, future catastrophes would be manifold. Performing regional seismic hazard as well as site response studies can possibly help in accurate estimation of probable future seismic scenario. Site class (SC) of EQ recording stations is an important part of both seismic hazard as well as site response analyses. In seismic hazard analysis, suitable attenuation relations are often selected based on comparison of recorded ground motion with proposed ground motion as per selected attenuation relation for the same SC. Thus, unless SC of recorded ground motions is known, suitability of selected attenuation relation cannot be validated. In addition, recent studies suggest that for same soil column, ground motion may amplify at the surface from minimal to very high depending upon input motion characteristics. Thus again, unless SC of recording station is not known, recorded ground motion cannot be considered with confidence as outcrop or base motion for region specific site response studies. In the present work, SC of eight

recording stations located in Tarai region of Uttarakhand, India located adjacent to the Himalayan belt and which are part of PESMOS database, are established by three different methods namely; equivalent linear ground response analysis, generalized inversion technique and horizontal to vertical spectral ratio method. Collectively all these three methods suggest same SC for each of the eight recording stations including Roorkee, Rishikesh, Dehradun etc. Further, obtained SC based on the present study is considerably different from available SC as per PESMOS database. However, present findings are matching with recent published work. Obtained results can be very helpful in developing surface seismic hazard using regional ground motion records towards minimizing future EQ induced damages.

**Keywords** GINV · HVSR · SHAKE2000 · Peak frequency · Site classification

## 1 Introduction

It has been widely acknowledged that surface geology and geotechnical characteristics at a site strongly influences the characteristics of earthquake (EQ) generated base motion by modifying its amplitude, frequency content and duration (Apostolidis et al. 2006; Walling et al. 2009; Kumar et al. 2016). This

---

N. Harinarayan · A. Kumar (✉)  
Department of Civil Engineering, Indian Institute of Technology Guwahati, Guwahati, Assam, India  
e-mail: abhiak@iitg.ernet.in

phenomenon known is local site effects and is a major factor responsible for the higher level of ground shaking occurring during an EQ at soil sites in comparison to adjacent rock sites (Mirzaoglu and Dýkmen 2003). Estimation of local site effect has become one of the major goals in EQ geotechnical engineering. Local site effect causes abnormal EQ damage patterns due to varying amplification of seismic waves by the local soil even within the epicentral region. Studies on the damage patterns witnessed during 1985 Michoacan EQ highlighted the importance of the local site effect among the scientific community. It was during this EQ that significant damages were observed in the city of Mexico located about 600 km away from the epicenter (Dobry et al. 2000). Later, Seed et al. (1988) concluded that this amplification in the ground shaking is due to local soil and not due to EQ source. During this EQ, ground motions between the bedrock and the surface were amplified up to five times due to significant impedance contrast between the bedrock and soil layers. Similarly, 2001 Bhuj EQ ( $M_w = 7.7$ ) is an excellent example of local site effect playing an important role in triggering damages at sites on soft soils. Ahmedabad, Bhuj, Rajkot, Anjar and Gandhidham cities spreading over 350 km away from the epicenter reported extensive damages to buildings (Verma et al. 2014). The dams at Fategadh, Kaswati, Suvi, and Tapar, built on alluvial soil also undergone damages (Krinitzsky and Hynes 2002). Instances reported above and many more are clear indications that local geology is responsible for severe damages during EQs, not only in the epicentral region but at farther distances as well.

For regions under moderate to high seismic hazard, estimation of true seismic hazard at the surface is a challenging problem. In general, surface seismic hazard can be divided into two parts namely; determination of seismic hazard at bedrock level and transfer of bedrock motion to the surface using ground response analysis. Accuracy of both; bedrock seismic hazard as well as regional site response analyses are significantly affected by regional ground motion records and site class (SC) of these recording stations. Attenuation relations correlates EQ and site characteristics with ground motion parameter. For developing countries like India with limited ground motion record available, regional attenuation relations based on recorded ground motions are still very limited

(Anbazhagan et al. 2013a). Development of region specific attenuation relation requires lot of recorded ground motions. In addition, correct SC of recording stations must be known in absence of which it will be difficult to understand whether proposed ground motion based on attenuation relation is at bedrock or at surface. Secondly, SC of recording station is very important in seismic hazard analysis. In case regional specific attenuation relations are not known, attenuation relations developed for other regions with similar seismic activity are often selected (Nath and Thingbaijam 2011; Anbazhagan et al. 2013b; Kumar et al. 2013). In order to validate selected attenuation relation for seismic hazard study, comparison between ground motion based on selected attenuation relation and the one recorded by the recording station are made. Majority of attenuation relations are developed for different SCs. However, if the SC of recording station is not known, recorded ground motions cannot be used for selection of suitable attenuation relation. This will have adverse effect of seismic hazard assessment and thus SC of recording stations should be known.

Recent literature suggests that same soil can cause low to high amplification of ground motion depending upon the amplitude and frequency content of input motion (Kumar et al. 2015, 2016, 2017; Mondal and Kumar 2015). This is indirectly a function of strain developed by the input motion in the soil layers (Kumar and Mondal 2017). Accuracy of a region specific site response analysis which consists of transfer of seismic hazard values from bedrock to the surface need ground motions at known site condition. Thus, unless SC of recording stations are not known correctly, there will be always an uncertainty that regional ground motion records should be suitably considered as bedrock motion or within soil. For this reason, most of the ground response studies conducted in India use ground motions recorded in other parts of the globe rather using regional ground motion records rather using available ground motion records.

Present study area of Tarai region lies close to the active Himalayas in Indo-Gangetic basin. As per IS 1893: 2002, the region comes under seismic zone IV and V clearly suggesting region of severe and very severe seismic activity and thus attempts to understand surface seismic hazard is of prime importance. There are significant numbers of recording stations installed in Tarai region which are maintained by PESMOS ([www.pesmos.in](http://www.pesmos.in)) under a Ministry of Earth Science

project entitled “National Strong Motion Instrumentation Network”. PESHOS is widely referred database for seismic hazard as well as regional ground response studies. However, inspection of the strong motion database of PESHOS indicates an ambiguity SC of the recording station given in PESHOS. As per Kumar et al. 2012, site classification used in PESHOS is based on physical description of surface materials, local geology following Siesmotectonic Atlas of India (GIS 2000), Geological Maps of Indian and not based on actual field investigation. Classification scheme used by PESHOS consists of three SCs in accordance with Borchardt (1994) namely; SC A ( $V_{s30} > 700$  m/s), SC B ( $375$  m/s  $< V_{s30} < 700$  m/s), and SC C ( $V_{s30} < 375$  m/s). SC A and SC B refer to firm/hard rock site and soft to firm rock site respectively and SC S refers to soil sites. Thus, PESHOS followed classification scheme is very broad. Pandey et al. (2016) highlighted this limitation in SC of various recording stations given by PESHOS. Importance of SC is already discussed above. In the present work, SC of eight recording stations in Tarai region are established using three different approaches namely GINV, HVSR and site response analysis as discussed in detail under subsequent headings.

## 2 Study Area

The Himalayan arc extending from Kashmir in the northwest to Arunachal Pradesh in the northeast, located between 75E and 98E with an approximate length of 2500 km was evolved as a result of collision of the Indian and the Eurasian plates which took place about 50 million years ago (Kayal 2001). The seismicity of the Himalayan belt is due to the continued convergence of the two continental plates which is approximately at the rate of 5 cm/year (Bilham 2016) resulting in uneven stress accumulation. The region is one of most the seismically active regions in the world having encountered four major EQs ( $M \geq 8.0$ ) in the past 120 years.

For the present work, strong motion recording stations located in the Tarai region of the State of Uttarakhand, India in the Western Himalayan segment is considered. All the eight recording stations considered in this study cover an area between 77°E and 80°E longitude and 28.5°N and 30.4°N latitude in the towns of Tanakpur, Roorkee, Haridwar, Rishikesh,

Uddham Singh Nagar, Khatima, Dehradun, Kashipur and Vikasnagar. Figure 1 shows the location of above recording stations while Table 1 presents the coordinates of each of the selected recording stations. Present study area is bounded by the Main Central Thrust (MCT) and the Main Boundary Thrust (MBT) (Valdiya 1980). As per available records, the region of Uttarakhand witnessed two moderate EQs in the recent past namely; 1991 Uttarakashi EQ ( $M_w = 6.8$ ) and 1999 Chamoli EQ ( $M_w = 6.6$ ). Evidences of local site effects in the damage patterns were observed during each of the above two EQs. As per Mahajan and Viridi (2001), 1991 Uttarakashi EQ caused severe damages to infrastructure, especially to the traditional houses in Rudraprayag, Chamoli and Tehri districts of Uttarakhand. Similarly, 1999 Chamoli EQ also reported extensive damages and caused 100 casualties injuring other hundreds (Verma et al. 2014). Prior to above two EQs, the present study area also witnessed other two devastating EQs in pre-instrumental times including the 1803 Kumaon-Nepal EQ ( $M = 7.5 +$ ) and the 1905 Kangra EQ ( $M_s = 7.8$ ). Dehradun, the capital of Uttarakhand falls in purview of the present study along with Hardwar and Rishikesh, regarded as one of the holiest places and major pilgrimage centers to Hindus. As per Census 2011, state of Uttarakhand has a population of 0.1 billion. Majority of the houses in the region are made up of materials like mud, brick and stones which can undergo major damage to complete damage during probable future EQ similar to past experiences as discussed earlier.

As per Kumar et al. (2012), significant number of EQ recording instruments were installed at several locations across Uttarakhand. Since SC of above recording stations are not known correctly, no to very few studies are available where ground motion recorded by these recording stations were used either for selection of attenuation relation for seismic hazard analysis or for regional site response studies. In the present work, attempts to establish SC of all eight recording stations located in the Tarai region from three different methods including GINV, HVSR and site response analysis are done. GINV is applied to the S-wave and Coda wave portions of the accelerogram separately, for all the eight recording stations thus giving a comparison of the S-wave and Coda wave spectral accelerations curves for the Uttarakhand region of the north-western Himalayas. It has to be

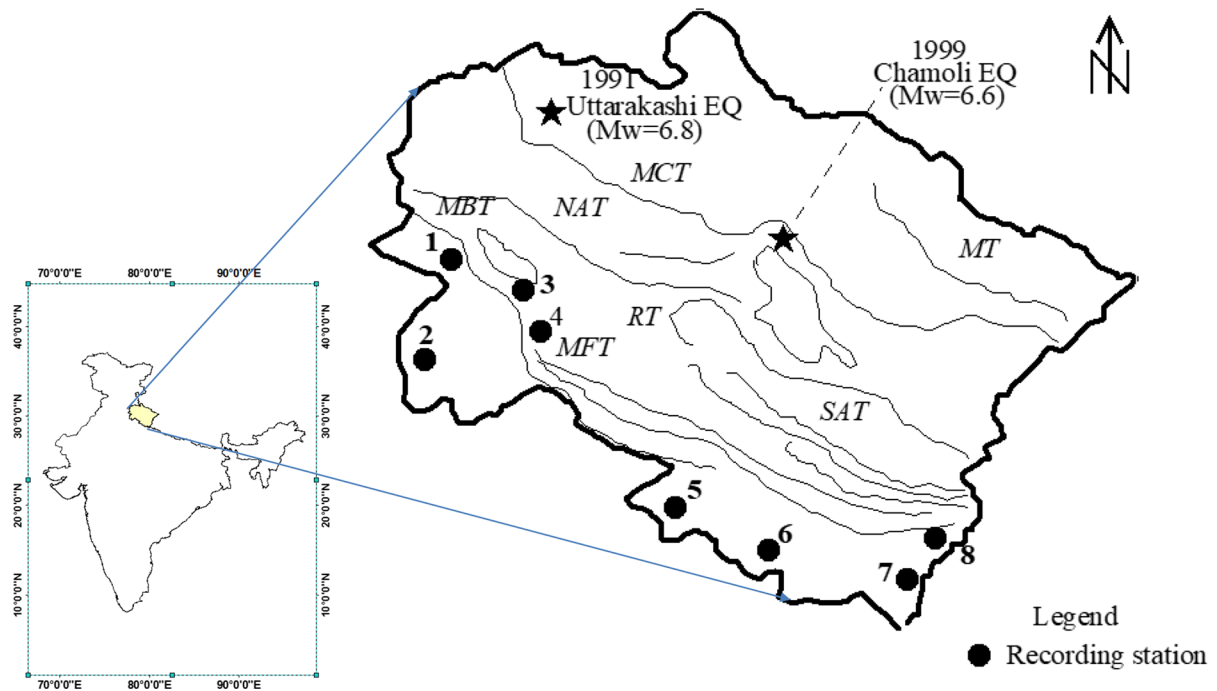


**Fig. 1** Study area showing eight recording stations considered for the present work [1-Dehradun; 2-Roorkee; 3-Rishikesh; 4-Vikasnagar; 5-Kashipur; 6-Udham Singh Nagar; 7-Khatima; 8-Tanakapur, MCT-Main Central Thrust, MBT-Main Boundary

Thrust, MFT-Main Frontal Thrust, RT-Ramgarh Thrust, MT-Martoli Thrust, SAT-South Almora Thrust and NAT-North Almora Thrust] (modified after Kumar et al. 2011)

**Table 1** Details of recording stations used in the present work

Recording Station (1)	Latitude (°) (N) (2)	Longitude (°) (E) (3)
Khatima	28.919	79.969
Udham Singh Nagar	28.997	79.403
Tanakpur	29.074	80.112
Kashipur	29.210	78.960
Roorkee	29.866	77.901
Rishikesh	30.116	78.281
Dehradun	30.316	78.042
Vikas Nagar	30.453	77.754

mentioned here that GINV is used without a reference site to generate average spectral acceleration curves based on north–south, east–west and vertical components of ground motion records at each of the eight recording stations. Further, SCs of all the eight recording stations are also computed using HVSR method. Since subsoil characteristics at these recording stations are known from previous works, in addition to GINV and HVSR, equivalent linear ground response analysis of recording stations are also done

using SHAKE2000 (Schnabel et al. 1972), to determine SCs of above recording stations.

### 3 Data Set

Accelerographs used for the recording ground motion, available in PESMOS consists of internal AC-63 GeoSIG triaxial force balanced accelerometers and GSR-18 GeoSIG 18 bit digitizers with external GPS (Kumar et al. 2012). During each EQ, ground motion recordings are done in trigger mode at a sampling rate of 200 samples per second. For the present analyses, the EQ records consists of ground motions recorded at the eight recording stations (Fig. 1) in the Tarai region of Uttarakhand are selected from PESMOS database. The database selected for the present analyses consist of 22 ground motions recorded during 12 EQ, with magnitudes ranging from 3.5 to 5 while focal depths ranges from 2 to 43 km. Table 2 summarizes the details of each EQs and the recording station at which ground motion during each EQ are available which are considered for the present work. All the EQ records

**Table 2** Strong motion records from Tarai region of Uttarakhand

Sl. No. (1)	Date (2)	Latitude (N) (3)	Longitude (°) (E) (4)	Magnitude (5)	Focal depth (km) (6)	Recording stations with ground motion available during EQs listed in column (2)														
						Khatima	Udham Singh Nagar	Tanakapur	Kashipur	Roorkee	Rishikesh	Dehradun	Vikasnagar							
1	22/07/2007	31.20	78.20	5.0	33.0				✓											
2	22/02/2010	30.00	80.10	4.7	2.0		✓													
3	14/03/2010	31.70	76.10	4.6	29.0															
4	05/01/2010	29.90	80.10	4.6	10.0															
5	05/03/2010	30.40	78.40	3.5	8.0															
6	28/05/2010	31.20	77.90	4.8	43.0															
7	20/06/2010	30.50	79.40	4.6	12.0		✓													
8	26/02/2011	29.60	80.80	4.3	10.0									✓						
9	04/04/2011	29.60	80.80	5.7	10.0		✓							✓						
10	03/05/2012	28.70	76.60	4.9	14.0															
11	23/08/2012	28.40	82.70	5.0	10.0															
12	01/09/2013	29.75	81.74	5.0	34.0															✓

consisted of uncorrected acceleration time histories which were corrected for baseline first following Kumar et al. (2012). A 5% cosine taper is then applied following a band pass filter between the frequency range 0.1 and 20.0 Hz using a Butterworth filter. Further, S-wave and coda wave portions of the accelerogram was separated following Kato et al. (1995) for GINV of S-wave and Coda wave in the present work.

#### 4 Methodology Used and Analyses

A number of analytical approaches are available for evaluating site characteristics of recording stations using available EQ records. Comparisons among various approaches were presented by Field and Jacob (1995), Parolai et al. (2004), Shoji and Kamiyama (2002) etc. and are not reported here. However, above literatures support that GINV technique and HVSR can give consistent information about site characteristics in terms of peak frequency ( $f_{peak}$ ). Detailed discussion on GINV and HVSR can be found in following sections.

##### 4.1 GINV

Andrews (1986) developed GINV technique by recasting the method of spectral ratio into a generalized inversion problem based on inverting the Coda wave spectra of the recorded EQ ground motions. Since then, various forms of this technique have been developed and used for estimating the seismic characteristics by various researchers (Castro et al. 1990; Boatwright et al. 1991; Oth et al. 2008 etc.). As per Iwata and Irikura (1988), spectral acceleration of the  $i$ th EQ recorded at the  $j$ th recording station,  $U(f)_{ij}$  can be represented in the frequency domain as the product of source term ( $S(f)_{ij}$ ), path attenuation ( $P(f)_{ij}$ ) and site term ( $G(f)_j$ ) as shown below;

$$U(f)_{ij} = S(f)_{ij}P(f)_{ij}G(f)_j \tag{1}$$

Further, effect of path attenuation from the spectral content of the record is removed following Andrews (1986) as:

$$U^A(f)_{ij} = \frac{U(f)_{ij}}{P(f)_{ij}} = S(f)_{ij}G(f)_j \tag{2}$$

This value of  $P(f)_{ij}$  for S wave and Coda wave can be determined using Eqs. 3a and 3b respectively as;

$$P(f)_{ij} = \frac{1}{R_{ij}} \left[ e^{\frac{-(\pi f R_{ij})}{Q_s(f)\beta}} \right] \text{ for S wave} \tag{3a}$$

$$P(f)_{ij} = \frac{1}{t} \left[ e^{\frac{-(\pi f t)}{Q_c(f)}} \right] \text{ for Coda wave} \tag{3b}$$

where,  $R$  is the hypocentral distance,  $f$  is the frequency,  $Q_s(f)$  is the quality factor for S wave,  $\beta$  is the average shear wave velocity of the crustal medium for the region,  $t$  is the lapse time and  $Q_c(f)$  is the quality factor of the Coda wave.

Equation 2 above can be linearized by taking natural logarithms on both sides as per Andrews (1986) giving;

$$\ln U^A(f)_{ij} = \ln S(f)_i + \ln G(f)_j \tag{4}$$

Further, multiply Eq. 4 on both sides by a weighted factor ( $\sigma_{ij}$ ) to impose a balance in the quality of the data with a need to include as many observations as possible. Thus,  $\sigma_{ij}$  is an estimate of the standard deviation of the data given by the ratio of the signal spectrum to a noise sample spectrum,  $N_{ij}(f)$  as prescribed by Andrews (1986) which can be determined as;

$$\sigma_{ij} = \frac{\max\left(\min\left(\frac{U_{ij}(f)}{N_{ij}(f)}, 5.0\right), 1.0\right)}{5} \tag{5}$$

It has to be mentioned that the value of  $\sigma_{ij}$  is limited to the range of 1.0–2.0 following Hartzell (1992).

Multiplying Eq. 4 by Eq. 5 will give;

$$\sigma_{ij} \ln S_i + \sigma_{ij} \ln G(f)_j = \sigma_{ij} \ln U^A(f)_{ij} \tag{6}$$

Considering:  $\sigma_{ij} \ln S_i = s_i(f)$ ,  $\sigma_{ij} \ln G(f)_j = g(f)$  and  $\sigma_{ij} \ln U^A(f)_{ij} = d_{ij}$

In matrix form, Eq. 6 can be written following the notations of Menke (1989) and in accordance with Joshi et al. (2010) as;

← 1 <sup>st</sup> event →				← n <sup>th</sup> event →				← site effect →					
1	2	...	m	1	2	...	m	1	2	...	m		
1	0	...	0	0	0	...	0	0	1	0	...	$s_1(f_1)$	$d_1(f_1)$
0	1	...	0	0	0	...	0	0	0	1	...	:	:
:	:	:	:	:	:	:	:	:	:	:	:	:	:
:	:	:	:	:	:	:	:	:	:	:	:	:	:
0	0	...	1	0	0	...	0	0	0	0	...	$s_1(f_n)$	$d_1(f_n)$
For n <sup>th</sup> earthquake												$s_n(f_1)$	$d_n(f_1)$
0	0	...	0	1	...	...	0	0	1	0	...	:	:
0	0	...	0	0	1	...	0	0	0	1	...	$s_n(f_n)$	$d_n(f_n)$
:	:	:	:	:	:	:	:	:	:	:	:	$g(f_1)$	$d_n(f_m)$
:	:	:	:	:	:	:	:	:	:	:	:	$g(f_2)$	:
:	:	:	:	:	:	:	:	:	:	:	:	:	:
0	0	...	0	0	0	...	0	1	0	0	...	$g(f_m)$	$d_n(f_m)$

(7)

For ‘m’ number of sample frequency and ‘n’ number of EQs recorded at a particular station, the above matrix form (Eq. 7) represents a purely indeterminate system since there are  $(n + 1) \times m$  unknowns for  $m \times n$  data. The above matrix is solved in this work using minimum norm inversion procedure similar to that of Joshi et al. (2010) such that  $S(f)_{ij}$  as well as  $G(f)_j$  can be determined at each of the selected recording stations. It has to be highlighted here that determination of source components is beyond the scope of the present work and thus only  $G(f)_{ij}$  is attempted in this work in terms of pseudo-spectral acceleration (PSA).

Based on the above discussed methodology, analyses are performed for east–west, north–south and vertical components separately to obtain the amplification curves for these components. The values of  $\beta$  is taken as 3.15 km/s and  $Q_s(f) = 174f^{1.27}$  are considered after Sharma et al., 2014 for the recording stations in Uttarakhand region. Further, the value of  $Q_c(f) = 126f^{0.95}$  given by Gupta et al. (1995) for the Garhwal Himalayas are used in this work. The value of  $\sigma_{ij}$  used in this study is calculated using Eq. 5 while  $N_{ij}(f)$  is

considered as the ground motion at 2 s just before the arrival of P wave. Based on findings from east–west and north–south components, one horizontal component is determined as the geometric mean of the two components. Further, ratio of this horizontal component to the above determined vertical component are estimated for each recording station. The value of frequency corresponding to the maximum value of above ratio is the peak frequency ( $f_{peak}$ ). The above procedure is carried out for the S wave and Coda wave portion of the ground motion to develop horizontal to vertical ratio versus frequency curve denoted by GINVS and GINVC respectively.

#### 4.2 HVSR

HVSR method was an extension of Nakamura (1989) technique used to estimate the subsoil characteristics using Horizontal to Vertical Fourier spectrum Ratio (HVFR) of recorded ambient noises. Nakamura (1989) work was based on the assumption that the soil amplification characteristics are retained only in the horizontal component while the source and the path

characteristics are maintained both in vertical as well as horizontal components of ground motion. However, highlighting the difficulty in identification of distinct peak in HVFR, Zhao et al. (2006) concluded that instead of considering ratio of horizontal to vertical records in terms of Fourier spectra, if HVSr in terms of spectral acceleration, for 5% damping is considered, it will have significant effect on smoothening. This way, a clear and distinct peak in the HVSr curve can be identified  $f_{\text{peak}}$  from any ground motion recorded at a recording station as discussed by Harinarayan and Kumar (2017a, b). HVSr method has been applied to EQ recordings worldwide (Luzi et al. 2011, Yaghmaei-Sabegh and Tsang 2011; Alessandro et al. 2012 etc.) to obtain the site characteristics in terms of the  $f_{\text{peak}}$ . Harinarayan and Kumar (2017a, b) attempted HVSr for 90 recording stations located in northwestern Himalayas including 8 recording stations used in this work. In the above work, HVSr for each recording station was determined using following steps;

1. Calculate the response spectra considering 5% damping value, for north–south, east–west and vertical components of ground motion records.
2. The response spectra of each component is smoothen using a Konno and Ohmachi (1998) window with a bandwidth parameter “b” of 20.
3. The geometric mean of the two horizontal response spectra components (H) is obtained using the Eq. (8);

$$H = (H_{\text{EW}} \times H_{\text{NS}})^{0.5}. \quad (8)$$

4. The ratio of H to V (H/V) is then calculated.

Here,  $H_{\text{EW}}$  and  $H_{\text{NS}}$  are the 5% damped pseudo response acceleration of the horizontal east–west and north–south components respectively and V is the 5% damped pseudo response acceleration of the corresponding vertical component. The HVSr at each station can be determined as;

$$(\text{HVSr})_i = \frac{\sum_{i=1}^{N_i} \frac{H}{V}}{N_i} \quad (9)$$

Here,  $N_i$  is the number of events recorded at station “I” and  $(\text{HVSr})_i$  is the average HVSr value for the station “i”. The  $f_{\text{peak}}$  for a particular station is the frequency corresponding to a maximum value of  $(\text{HVSr})_i$ .

### 4.3 Ground Response Analysis Using SHAKE2000

In addition to above two methods, one dimensional equivalent ground response analyses are also carried in this work to obtain the spectral amplification curves for each of the eight recording stations. In general, EQ records at bedrock or outcrop from a particular region are used in region specific ground response analysis as input to have a region specific site response analysis. For the Tarai region however, Pandey et al. (2016) based on MASW studies reported that the recording stations are located on soil sites. It has to be mentioned here that recording stations considered by Pandey et al. (2016) have eight recording stations common to the present work. Therefore unlike GINV, EQ records from these recording stations cannot be used for site specific ground response analysis. In such a case, a more appropriate alternate is the use of ground motions during any EQ which is also considered in GINV and HVSr above, but recorded at nearby rock site condition as bedrock motion. Sharma et al. (2014) carried out empirical and numerical studies using the EQ records from strong motion recording stations in the Garhwal region of Uttarakhand. Based on the findings by Sharma et al. (2014), Munsyari recording station was identified as rock site having  $f_{\text{peak}}$  of 7.1 Hz. For the present study, EQ event of 19/08/2008 of (M- 4.7), recorded at Munsyari recording station in Garhwal region of Uttarakhand is selected for input motions referring to the findings by Sharma et al. (2014). In here, two ground motions are considered for ground response analyses. While one ground motion is corresponding to vertical component of above EQ record, second component is the north–south component. Both of these ground motions are shown in Fig. 2.

In addition to input motion, site specific subsoil characteristics are also needed for ground response analysis. For all the eight recording stations considered under GINV and HVSr as discussed earlier, shear wave velocity variation with depth are taken from Pandey et al. (2016) as subsoil characteristics. Other important inputs in ground response analyses are modulus reduction ( $G/G_{\text{max}}$ ) curve and damping ratio ( $\beta$ ) curve. For recording stations considered in this work,  $G/G_{\text{max}}$  and  $\beta$  curves are selected referring to the work by Pandey et al. (2016). Based on the above selected input motions, subsoil characteristics,



**Fig. 2** Acceleration time history of EQ used as input motion for SHAKE2000 analysis

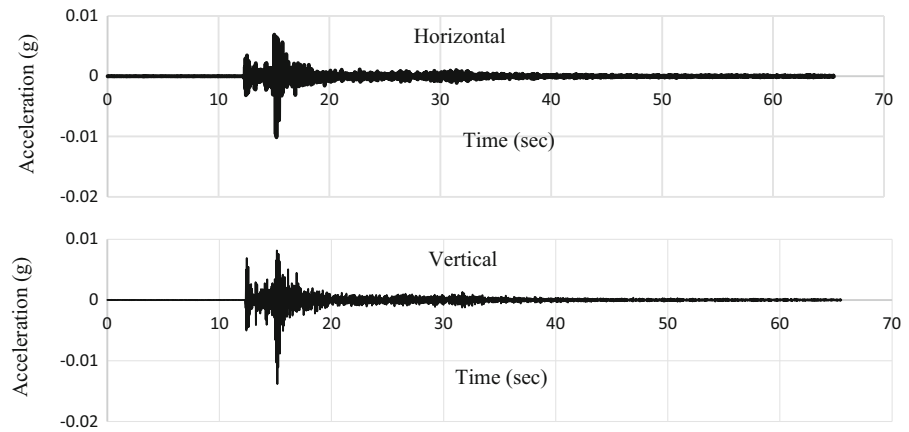


**Table 3** NEHRP site classification (BSSC, 2003)

Site class	Profile type	Shear wave velocity (m/s)	Fundamental frequency (Hz)
A	Hard rock	> 1500	> 12.71
B	Rock	760–1500	6.35–12.70
C	Very dense soil and soft rock	360–760	3.05–6.35
D	Stiff soil	180–360	1.52–3.05
E	Soft soil	< 180	< 1.52

$G/G_{max}$  and  $\beta$  curves, equivalent linear analyses using SHAKE2000 are performed separately for horizontal and vertical component at each of the recording station in terms of PSA. Further, site characteristics of each of the recording stations are assessed based on  $f_{peak}$  value. This value of  $f_{peak}$  is obtained from the ratio of the surface response spectra obtained using horizontal component of input motion to surface response spectra obtained using vertical component as discussed in the next section (Table 3).

### 5 Results and Discussion

In the following section, the site amplification obtained using GINV S, GINV C, SHAKE2000 analyses and HVSR are compared. It has to be mentioned here that initially the results of GINV S, GINV C and SHAKE2000 analyses are discussed for horizontal and vertical components separately. Later, the results of horizontal to vertical ratio of GINV S, GINV C and SHAKE2000 analyses are compared with HVSR curves.

Figure 3a–p shows the PSA curves estimated using GINV S (indicated by dotted lines), GINV C (indicated by dashed lines) referring to Eq. 6 and SHAKE2000 analyses (indicated by solid line) for horizontal and vertical components separately for each of the recording stations. It can be observed from Fig. 3a–p that for majority of the recording stations, PSA curves show similar variation trends based on GINV S, GINV C and SHAKE2000 for horizontal as well as vertical components. In addition, the values of predominant frequencies (corresponding to maximum amplification) based on GINV S, GINV C and SHAKE2000 analyses are closely matching for all the recording stations. The value of amplification obtained by the three methods are however not matching. Large discrepancies in the values of amplification based on GINV S and GINV C methods can be seen in Fig. 3a–p. Similar behavior was also reported by Margheriti et al. (1994), Field (1996) and Bonilla et al. 1997. It has to be mentioned here that Fig. 3a–p are produced just to show similarity between findings from GINV S, GINV C and SHAKE2000 in terms of variation pattern. SC of the recording stations, which

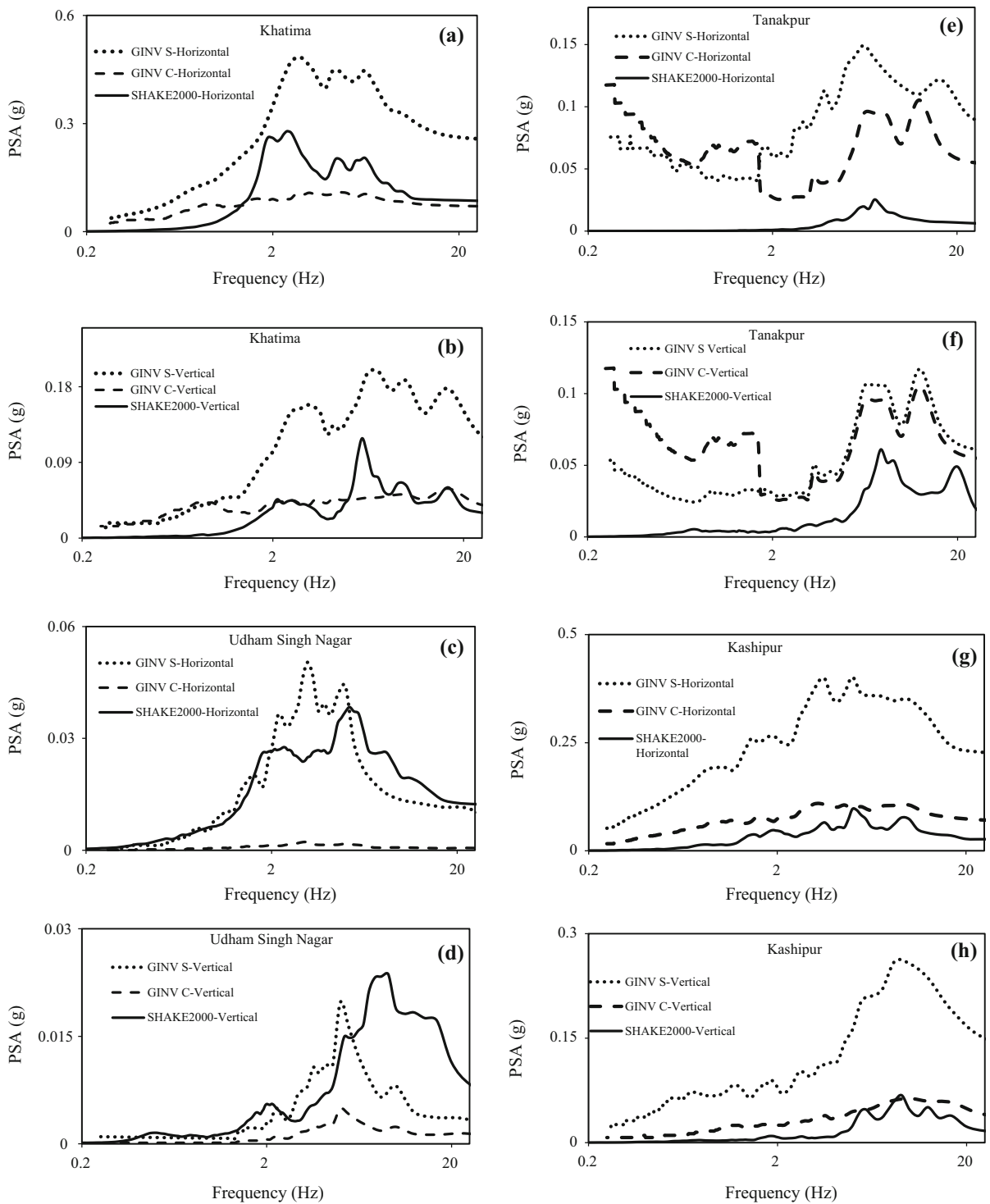


**Fig. 3** Site amplification curves obtained using GINV S, GINV C and SHAKE2000 analysis for horizontal component and vertical component

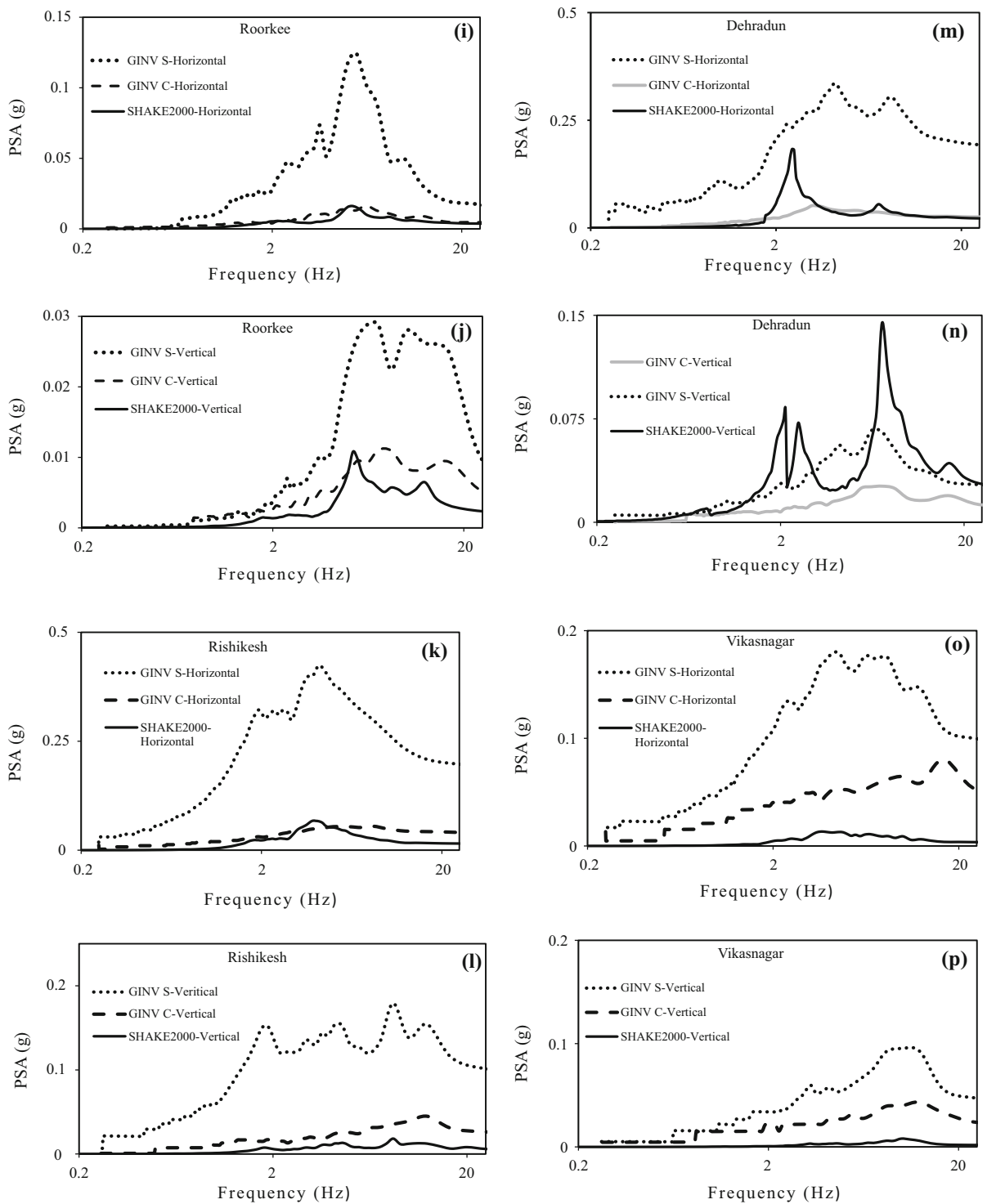
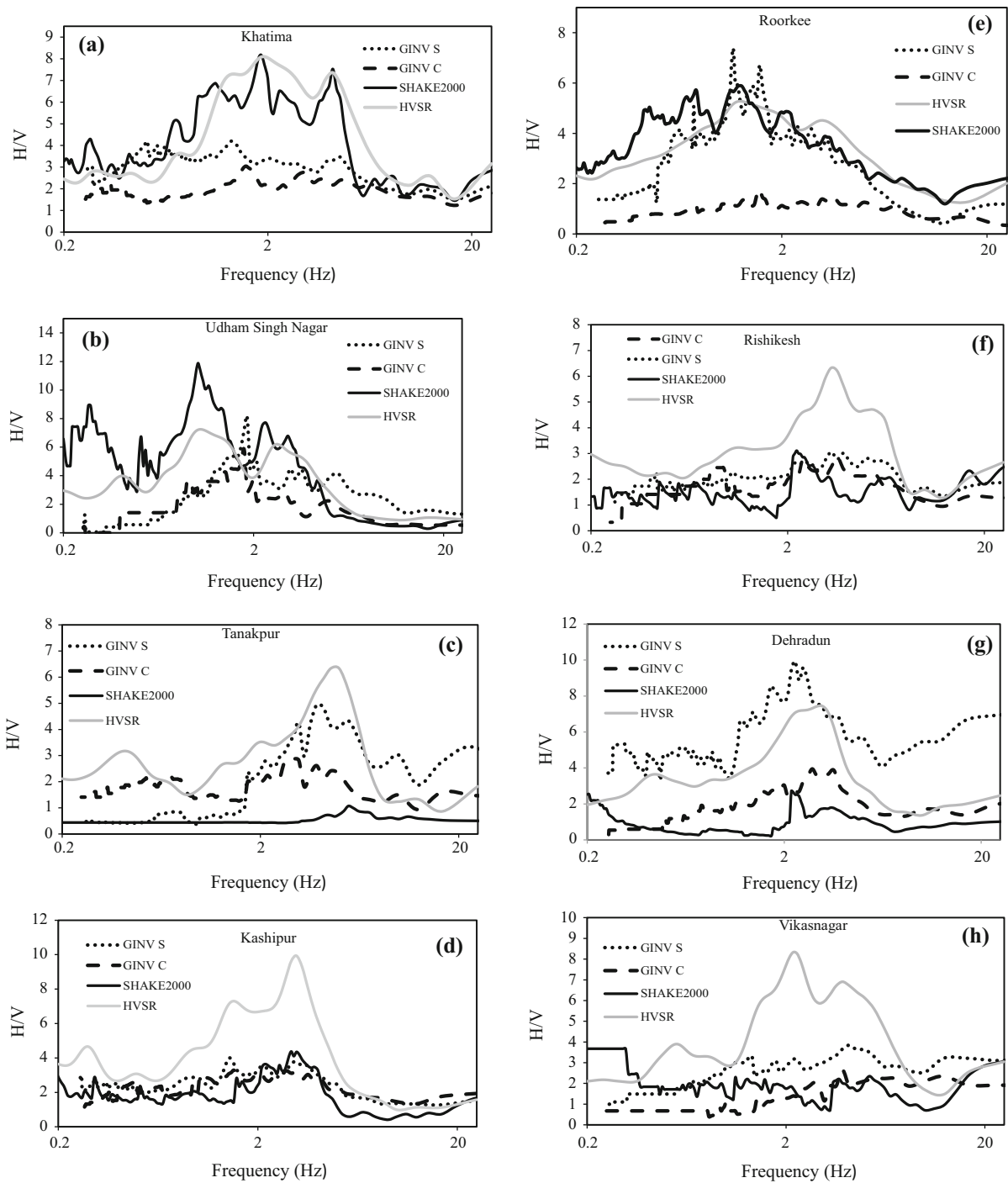


Fig. 3 continued



**Fig. 4** Horizontal to vertical ratio curve obtained using GIN V S, GIN V C, SHAKE2000 analysis and HVSr method

is the objective of present work however is a function of  $f_{peak}$  (which is estimated later) and not the value of amplification.

Based on above analyses, plots of the ratio of horizontal to corresponding vertical PSA curves for each of the recording station are shown in Fig. 4a–h.

**Table 4** Summary of  $f_{peak}$  and  $A_{peak}$  obtained using GINVS, GINVC, SHAKE2000 and HVSR

Recording stations	GINV S		GINV C		SHAKE2000		HVSR		Average	
	$f_{peak}$ (Hz)	$A_{peak}$	$f_{peak}$ (Hz)	$A_{peak}$	$f_{peak}$ (Hz)	$A_{peak}$	$f_{peak}$ (Hz)	$A_{peak}$	$f_{peak}$ (Hz)	$A_{peak}$
Khatima	1.50	4.02	1.61	2.96	1.92	8.10	1.85	8.20	1.72	5.82
Udham Singh Nagar	1.90	8.09	1.80	5.83	1.10	11.80	1.20	7.20	1.50	8.23
Tanakpur	3.80	4.93	2.94	2.87	5.50	0.99	4.50	6.34	4.18	3.78
Kashipur	1.56	3.95	1.58	3.65	3.22	4.22	3.12	9.93	2.37	5.44
Roorkee	1.40	7.30	1.70	1.80	1.50	6.00	1.56	5.40	1.54	5.12
Rishikesh	3.05	3.00	2.50	2.70	2.30	2.98	3.20	6.20	2.76	3.72
Dehradun	2.27	9.90	2.70	3.90	2.30	2.42	2.90	2.50	2.54	4.68
Vikasnagar	4.20	3.80	3.80	2.70	3.80	2.50	2.50	8.00	3.57	4.25

As seen in Fig. 4a–h, horizontal to vertical ratio curves for GINVS (indicated by dotted lines), GINVC (indicated by dashed lines) and SHAKE2000 (indicated by solid line) analyses are presented along with HVSR (indicated by solid line with lighter shade) for all eight recording stations. It can be observed from Fig. 4a–h that the curves obtained using the above four methods give clear peaks in terms of the maximum value of horizontal to vertical ratio (denoted as  $A_{peak}$ ). The range of  $A_{peak}$  varies between 1.17 and 9.9 based on all the four methods among all the recording stations as listed in Table 4. Further,  $A_{peak}$  value obtained using GINVS are lower compared to those obtained using GINVC. In comparison to GINVS, GINVC and SHAKE2000 analyses, HVSR based curves give higher values of  $A_{peak}$  except for Udham Singh Nagar, Roorkee and Dehradun. Previous works by Sharma et al. (2014), Field and Jacob (1995) and many others also reported that HVSR overestimate  $A_{peak}$ . Overall, all the curves shown in Fig. 4a–h show different  $A_{peak}$  variation based on all the above four methods. The value of  $A_{peak}$  is a function of input ground motion (Kumar et al. 2016, 2017) and thus can vary among all the above four methods as each method is based on different ground motions. It has to be mentioned here that GINVS and GINVC techniques for a particular recording station give average amplification curve (thus average  $A_{peak}$ ) for all the EQ used in the analyses as discussed earlier based on S wave and Coda wave parts of ground motion. On the other hand, SHAKE2000 analyses gives the amplification curve corresponding to selected single input ground motion. These might be the attributes for the

difference in the  $A_{peak}$  variation from GINVS, GINVC and SHAKE2000 as can be observed from Fig. 4a–h. Further, it has to be mentioned here again that the present work proposes SC for the recording station which is the function of  $f_{peak}$  and thus difference in  $A_{peak}$  variation from above methods are not going to affect the findings of the present work.

Again from Fig. 4a–i, the similar values of  $f_{peak}$  can be observed based on each of the above four methods. The value of  $f_{peak}$  based on all the four methods along with the average  $f_{peak}$  value ( $f_{peak}^{av}$ ) which is the average of  $f_{peak}$  values from all four methods, for all the eight recording stations are given in Table 4. Value of  $f_{peak}^{av}$  ranges between 1.80 and 4.18 Hz for all the recording stations. Based on the  $f_{peak}^{av}$ , corresponding value of average shear wave velocity for 30 m depth ( $V_{s30}$ ) is calculated for all the eight recording stations using the Eq. 10 (Kramer (1996), for a single layer model over half space.

$$V_{s30} = f_{peak}^{av} 4H \tag{10}$$

Here, H is the soil depth (taken as 30 m in this work for site classification). Further, the value of  $V_{s30}$  obtained in the present study (Column 2, Table 4) is compared with the value of  $V_{s30}$  obtained from MASW tests reported by Pandey et al. (2016) (Column 3, Table 4) for all the eight recording stations. It can be observed from Table 4 that  $V_{s30}$  obtained in the present study is in close range with findings of Pandey et al. (2016). Further site classification of the eight recording stations is carried out using above computed  $V_{s30}$  values as per site classification scheme followed by PESMOS (Column 5, Table 4). Further, obtained SC

**Table 5** Summary of shear wave velocity and site class as per PSMOS and NEHRP classification

Recording Station (1)	$V_{S30}$ from present study (2)	$V_{S30}$ from Pandey et al. (2016) (3)	Site class		
			Given in PSMOS (4)	Site class as per PSMOS classification scheme based on $V_{S30}$ calculated from $f_{peak}^{av}$ obtained from the present study (5)	NEHRP based site class (6)
Khatima	206.40	218	C	C	D
Udham Singh Nagar	180.00	198	C	C	D
Tanakapur	502.20	434	C	B	C
Kashipur	284.55	208	C	C	D
Roorkee	184.80	218	C	C	D
Rishikesh	331.50	305	C	C	D
Dehradun	305.10	289	C	C	D
Vikasnagar	429.00	425	C	B	C

are compared with the SC given in PSMOS (Column 4, Table 5) for above recording stations. According to the SC given in PSMOS, all the above recording stations belong to SC C. However, based on the present study, Tanakapur and Vikasnagar stations belong to SC B. The revised SC as per PSMOS classification for the eight recording stations are given in Column 5, Table 5.

The drawback of classification scheme used by PSMOS has already been discussed earlier. In addition to the above mentioned classification scheme, SC based on widely followed National Earthquake Hazards Reduction Program (NEHRP) classification scheme (Table 5) is also estimated for the eight recording stations. Based on the present study, recording stations at Tanakapur and Vikasnagar are classified as SC C while recording stations at Khatima, Udham Singh Nagar, Rishikesh, Kashipur, Roorkee and Dehradun are classified as SC D (Column 6, Table 4) based on NEHRP site classification scheme.

## 6 Conclusion

In the present study, SC for the eight seismic recording stations located in the Tarai region of Uttarakhand is carried using GINV, SHAKE2000 and HVSR methods. GINV is carried out for the S wave and the coda wave portion of the accelerogram separately. Further, SHAKE2000 analyses are done for above recording

stations using regional record from rock site. Amplification curves generated using GINV S, GINV C and SHAKE2000 show similar frequency dependent trend for both horizontal and vertical components for each of the recording station. Horizontal to vertical ratio versus frequency curves developed based on the obtained amplification curves along with the HVSR curves gives similar value of  $f_{peak}$  at each of the recording station. The value of  $V_{S30}$  for each recording station is computed using  $f_{peak}^{av}$  obtained from the present study and is found closely matching with field study available in the literature for all the eight recording stations. Further, SC of eight recording stations is attempted as per PSMOS followed classification scheme. Comparing the SC given by PSMOS with the results of the present study shows a mismatch in SC for Tanakapur, and Vikasnagar stations. This study again clearly indicates that the site classification given by PSMOS is not based on subsoil characteristics. Further, SC based on NEHRP classification scheme for all the eight recording stations is also carried out using above estimated  $V_{S30}$  values. Once SC of these recording stations are known from this work, ground motion recorded at above recording stations can be confidently used while developing attenuation relation for different SCs in the future.

Revised SC as well as NEHRP based SC proposed in this work might be very helpful for the use of ground motion records from the recording stations at Tarai

region of Uttarakhand to arrive at surface seismic hazard in the future.

**Acknowledgements** Authors are thankful for the PESMOS, Department of Earthquake Engineering for providing ground motion records used in the present work. In absence of recorded ground motion, carrying out present work would be impossible. The authors would also like to thank the INSPIRE Faculty program by the Department of Science and Technology (DST), Government of India for the funding project “Propagation path characterization and determination of in situ slips along different active faults in the Shillong Plateau” ref. no. DST/INSPIRE/04/2014/002,617 [IFA14-ENG-104] for providing necessary motivation and support for the present study.

## References

- Alessandro C, Bonilla LF, Boore DM, Rovelli A, Scotti O (2012) Predominant-period site classification for response spectra prediction equations in Italy. *Bull Seismol Soc Am* 102(2):680–695
- Anbazhagan P, Kumar A, Sitharam TG (2013a) Ground motion prediction equation considering combined dataset of recorded and simulated ground motions. *Soil Dyn Earthq Eng* 53:92–108
- Anbazhagan P, Smitha CV, Kumar A, Chandran D (2013b) Estimation of design basis earthquake using region-specific  $M_{max}$ , for the NPP site at Kalpakkam, Tamil Nadu, India. *Nucl Eng Des* 259(41):64
- Andrews DJ (1986) Objective determination of source parameters and similarity of earthquakes of different size. In: American Geophysical Union, Washington, pp 259–268
- Apostolidis PI, Raptakis DG, Pandi KK, Manakou MV, Ptilakis KD (2006) Definition of subsoil structure and preliminary ground response in Aigion city (Greece) using microtremor and earthquakes. *Soil Dyn Earthq Eng* 26(10):922–940
- Bilham R (2016) Himalayan Earthquakes. <http://cires1.colorado.edu/~bilham/indexHimEq.html>. Accessed 23 August 2016
- Boatwright J, Fletcher JB, Fumal TE (1991) A general inversion scheme for source, site, and propagation characteristics using multiply recorded sets of moderate-sized earthquakes. *Bull Seismol Soc Am* 81(5):1754–1782
- Bonilla LF, Steidl JH, Lindley GT, Tumarkin AG, Archuleta RJ (1997) Site amplification in the San Fernando Valley, California: variability of site-effect estimation using the S-wave, coda, and H/V methods. *Bull Seism Soc Am* 87(3):710–730
- Borcherdt RD (1994) Estimates of site-dependent response spectra for design (methodology and justification). *Earthq Spectra* 10:617–653
- Building Seismic Safety Council, B. S. S. C. (2003) NEHRP recommended provisions for seismic regulations for new buildings and other structures. Report FEMA-450 (Provisions), Federal Emergency Management Agency (FEMA), Washington
- Castro RR, Anderson JG, Singh SK (1990) Site response, attenuation and source spectra of S waves along the Guerrero, Mexico, subduction zone. *Bull Seismol Soc Am* 80(6A):1481–1503
- Dobry R, Borcherdt RD, Crouse CB, Idriss IM, Joyner WB, Martin GR, Power MS, Rinne EE, Seed RB (2000) New site coefficients and site classification system used in recent building seismic code provisions. *Earthq Spectra* 16(1):41–67
- Field EH (1996) Spectral amplification in a sediment-filled valley exhibiting clear basin-edge induced waves. *Bull Seismol Soc Am* 86:991–1005
- Field EH, Jacob KH (1995) A comparison and test of various site-response estimation techniques, including three that are not reference-site dependent. *Bull Seismol Soc Am* 85(4):1127–1143
- Gupta SC, Singh VN, Kumar A (1995) Attenuation of coda waves in the Garhwal Himalaya, India. *Phys Earth Planet Inter* 87(3–4):247–253
- Harinarayan NH, Kumar A (2017a) Determination of NEHRP site class of seismic recording stations in the northwest Himalayas and its adjoining area using HVSR method. *Pure Appl Geophys*. <https://doi.org/10.1007/s00024-017-1696-6>
- Harinarayan NH, Kumar A (2017b) Site classification of the strong motion stations of Uttarakhand, India, based on the model horizontal to vertical spectral ratio. In: Proceedings of geotechnical frontiers, GSP 281, Orlando, Florida, (ASCE special Publication)
- Hartzell SH (1992) Site response estimation from earthquake data. *Bull Seismol Soc Am* 82:2308–2327
- IS 1893 (2002) General provisions and buildings: criteria for earthquake resistant design of structures. Bureau of Indian Standards, New Delhi
- Iwata T, Irikura K (1988) Source parameters of the 1983 Japan Sea earthquake sequence. *J Phys Earth* 36(4):155–184
- Joshi A, Mohanty M, Bansal AR, Dimri VP, Chadha RK (2010) Use of spectral acceleration data for determination of three-dimensional attenuation structure in the Pithoragarh region of Kumaon Himalaya. *J Seismol* 14(2):247–272
- Kato K, Aki K, Takemura M (1995) Site amplification from coda waves: validation and application to S-wave site response. *Bull Seismol Soc Am* 85(2):467–477
- Kayal JR (2001) Microearthquake activity in some parts of the Himalaya and the tectonic model. *Tectonophysics* 339(3):331–351
- Konno K, Ohmachi T (1998) Ground motion characteristics estimated from spectral ratio between horizontal and vertical components of microtremor. *Bull Seismol Soc Am* 88(1):228–241
- Kramer SL (1996) Geotechnical earthquake engineering. *Engineering* 6:653
- Krinitzsky EL, Hynes ME (2002) The Bhuj, India, and earthquake: lessons learned for earthquake safety of dams on alluvium. *Eng Geol* 66:163–196
- Kumar A, Mondal JK (2017) Newly developed MATLAB based code for equivalent linear site response analysis. *Geotech Geol Eng* 35(5):2303–2325
- Kumar P, Kumar A, Sinval A (2011) Assessment of seismic hazard in Uttarakhand Himalaya. *Disaster Prev Manag Int J* 20(5):531–542
- Kumar A, Mittal H, Sachdeva R (2012) Indian strong motion instrumentation network. *Seismol Res Lett* 83(1):59–66

- Kumar A, Anbazhagan P, Sitharam TG (2013) Liquefaction hazard mapping of Lucknow—a part of Indo-Gangetic Basin (IGB). *Int J Geotech Earthq Eng* 4(1):17–41
- Kumar A, Harinarayan NH, Baro O (2015) High amplification factor for low amplitude ground motion: assessment for Delhi. *Disaster Adv.* 8(12):1–11
- Kumar A, Baro O, Harinarayan NH (2016) Obtaining the surface PGA from site response analyses based on globally recorded ground motions and matching with the codal values. *Nat Hazards* 81(1):543–572
- Kumar A, Harinarayan NH, Baro O (2017) Nonlinear soil response to ground motions during different earthquakes in Nepal, to arrive at surface response spectra. *Nat Hazards* 87(1):13–33
- Luzi L, Puglia R, Pacor F, Gallipoli MR, Bindi D, Mucciarelli M (2011) Proposal for a soil classification based on parameters alternative or complementary to  $V_{s30}$ . *Bull Seismol Soc Am* 9(6):1877–1898
- Mahajan AK, Virdi NS (2001) Macroseismic field generated by 29 March, 1999 Chamoli earthquake and its seismotectonics. *J Asian Earth Sci* 19:507–516
- Margheriti L, Wennerberg L, Boatwright J (1994) A comparison of coda and S-wave spectral ratio estimates of site response in the southern San Francisco Bay area. *Bull Seismol Soc Am* 84:1815–1830
- Menke W (1989) *Geophysical data analysis: discrete inverse theory*. Academic Press, New York
- Mirzaoglu M, Dýkmen U (2003) Application of microtremors to seismic microzoning procedure. *J Balkan Geophys Soc* 6(3):143–156
- Mondal JK, Kumar A (2015) Impact of frequency content of input motion upon local site effect. In: *Proceedings of Indian geotechnical conference, 17–19 Dec, COEP Pune, Maharashtra*
- Nakamura Y (1989) A method for dynamic characteristics estimation of subsurface using microtremor on the ground surface. *Railway Technical Research Institute, Quarterly Reports*, 30(1)
- Nath SK, Thingbaijam KKS (2011) Peak ground motion predictions in India: an appraisal for rock sites. *J Seismol* 15(2): 295–315
- Oth A, Bindi D, Parolai S, Wenzel F (2008) S-wave attenuation characteristics beneath the Vrancea region in Romania: new insights from the inversion of ground-motion spectra. *Bull Seismol Soc Am* 98(5):2482–2497
- Pandey B, Jakka RS, Kumar A (2016) Influence of local site conditions on strong ground motion characteristics at Tarai region of Uttarakhand, India. *Nat Hazards* 81(2):1073–1089
- Parolai S, Bindi D, Baumbach M, Grosser H, Milkereit C, Karakisa S, Zünbül S (2004) Comparison of different site response estimation techniques using aftershocks of the 1999 Izmit earthquake. *Bull Seismol Soc Am* 94(3):1096–1108
- Schnabel PB, Lysmer J, Seed HB (1972) SHAKE—a computer program for earthquake response analysis of horizontally layered sites. Report No. EERC 72-12, University of California, Berkeley
- Seed HB, Romo MP, Sun JI, Jaime A, Lysmer J (1988) The Mexico earthquake of September 19, 1985—relationships between soil conditions and earthquake ground motions. *Earthq Spectra* 4(4):687–729
- SEISAT (2000) *Seismotectonic Atlas of India and its Environs*, published by Geological Survey of India
- Sharma J, Chopra S, Roy KS (2014) Estimation of source parameters, quality factor (QS), and site characteristics using accelerograms: Uttarakhand Himalaya region. *Bull Seismol Soc Am* 04(1):360–380
- Shoji Y, Kamiyama M (2002) Estimation of local site effects by a generalized inversion scheme using observed records of ‘Small-Titan’. *Soil Dyn. Earthq. Eng.* 22(9):855–864
- Valdiya KS (1980) *Geology of Kumaun lesser Himalaya*. Wadia Institute of Himalayan Geology, Dehradun
- Verma M, Singh RJ, Bansal BK (2014) Soft sediments and damage pattern: a few case studies from large Indian earthquakes vis-a-vis seismic risk evaluation. *Nat Hazards* 74:1829–1851
- Walling MY, Mohanty WK, Nath SK, Mitra S, John A (2009) Microtremor survey in Talchir, India to ascertain its basin characteristics in terms of predominant frequency by Nakamura’s ratio technique. *Eng Geol* 106:123–132
- Yaghmaei-Sabegh S, Tsang HH (2011) A new site classification approach based on neural networks. *Soil Dynam Earthquake Eng* 31(7): 974–981
- Zhao JX, Irikura K, Zhang J, Fukushima Y, Somerville PG, Asano A, Ohno Y, Oouchi T, Takahashi T, Ogawa H (2006) An empirical site-classification method for strong-motion stations in Japan using H/V response spectral ratio. *Bull Seismol Soc Am* 96:914–925